Proceedings of 2004 IEEE/RSJ International Conference on
Intelligent Robots and Systems
September 28 - October 2, 2004, Sendai, Japan

Transient Analysis of Bar-type Ultrasonic Motors

Yosuke Nakagawa
Dept. of Mechanical Engineering
Keio University
Yokohama, Japan
y09560@educ.cc.keio.ac.jp

Akira Saito
Dep. of Mechanical Engineering
Michigan University, Ann Arbor
Michigan, U.S.A.
asakira@umich.educ

Takashi Maeno
Dep. of Mechanical Engineering
Keio University
Yokohama, Japan
maeno@mech.keio.ac.jp

Abstract— **In this paper, analysis of the dynamics of the ultrasonic motors is introduced. Though static characteristics have in the past been clarified, the dynamic characteristics were still unclear. For the purpose of realizing high speed control of ultrasonic motors, we analyzed the dynamic characteristics through measurement and numerical simulation. Among the different types of ultrasonic motors, we focused on bar-type ultrasonic motors and first measured the step response using a laser doppler velocimeter (LDV). We measured changing the input parameters and showed the relationship between input parameters and delay, overshoot of the rotational speed of the rotor. Next, we established a mathematical model of the bar-type ultrasonic motor. In our model, we approximated the stator as a rigid disc and torsional spring. We set the discrete spring at the contact area between rotor and stator, and simulated considering stick-slip at the contact area. The results of numerical simulation matched that of the measurements qualitatively and we clarified the dynamics of the contact condition and friction force at the contact area.**

Keywords- Ultrasonic motor, transient analysis, mathematical model, stick-slip condition

I. INTRODUCTION

Recently robotics has shown great progress. There are bipedal walking robots, and robot hands that can accomplish dexterous handling. These robots can complete sophisticated tasks with precision. Though, the motion of these robots is not fast enough. In navigating system, robots are required to be high response to commands, therefore high speed control of robots are needed. Most actuators used in these devices are the electromagnetic motors. They are beneficial cost-wise, for the easiness to control and longstanding experiences in their industry. However when considering electromagnetic motors as actuators for robots that move fast, they have some major weaknesses. First is the low response caused by the large inertia of the gear-train. Inaccuracy is the second issue which occurs due to the existence of gear-trains. It is difficult to solve these problems with existing technologies, and new actuators superseding electromagnetic motors are needed.

Ultrasonic motors are actuators driven by ultrasonic vibrations and friction force. They have advanced features such as low-speed and high-torque, high response, silence, and compact size. They are utilized for robot hand that realizes high response with rising time of about 100ms[1].

Recently, numbers of researchers of ultrasonic motors have been clarified the static characteristics, and able to control considering their non-linear characteristics [2][3]. On the other hand, their dynamic characteristics have yet to be analyzed and high speed control of ultrasonic motors has not been realized. Some researchers have established the mathematical models and estimated the dynamic characteristics [4][5]. However, measurements are not conducted and the adequacy of the simulation is not shown. Furthermore, the prospects of the contact problem are not taken to consideration in these papers. Friction force caused by contact between the rotor and stator is the driving force of ultrasonic motors and its contact problem is very important [6][7][8]. Therefore the dynamics of the contact conditions have to be calculated.

In this paper, we analyze the dynamics of ultrasonic motors by measurement and numerical simulation in order to realize higher speed control of robot hands using ultrasonic motors.

II. BAR-TYPE ULTRASONIC MOTOR

We focused on bar-type ultrasonic motors for this study. Fig. 1 shows the structure. Bar-type ultrasonic motors are composed of a rotor and stator, and are pressed by a spring. When we apply an alternate current voltage to the piezoelectric ceramics sandwiched in the stator, two first modes of bending vibrations orthogonal to each other occur within the stator. Shifting their phase 90deg, nutation (traveling wave) generates at the top of the stator. The friction force is generated between the rotor and the stator, and the rotor is driven by the friction force. Ultrasonic motor performance depends on the applied voltage. Frequency, amplitude, and phase difference also affects the performance of the motor.

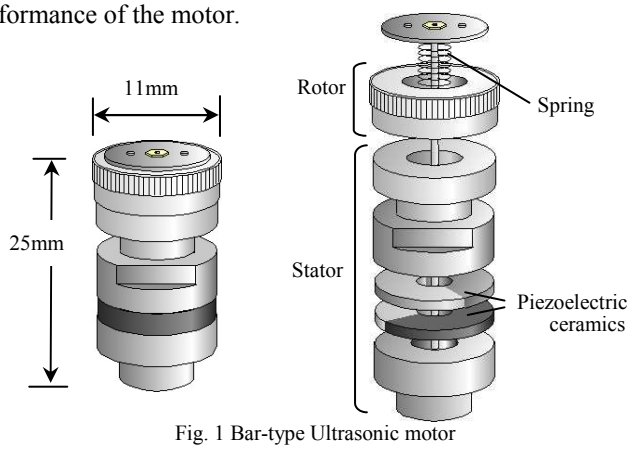

Fig. 1 Bar-type Ultrasonic motor

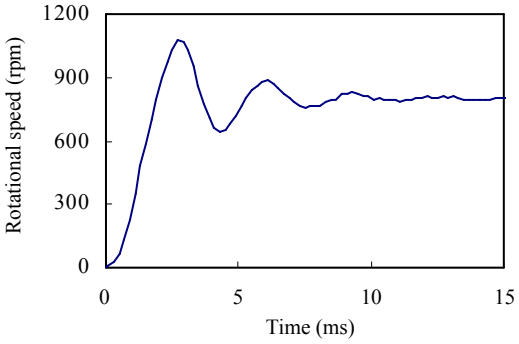

Fig. 2 Measured history of the rotational speed

III. MEASUREMENT

In this section, measurement of the step response of the bar-type ultrasonic motor is described. We measured the history of the rotational speed of the rotor using a laser doppler velocimeter (LDV) when we applied an alternate current voltage as a step input. Fig. 2 shows the result when we applied voltage with frequency, amplitude, and phase difference of 37.1kHz, 15Vp-p and 90deg. The rotational speed of the rotor increases in 3ms and settle in 10ms. There is the overshoot and the curve matches that of the step response in the second order lag system. The step response of an electromagnetic motor is the first order lag system, therefore the system of the ultrasonic motor is different from that of the electromagnetic motor. This is attributed to the driving principle of ultrasonic motors. Ultrasonic motors are driven by the friction force caused by vibration of the stator. The system of the stator is second order lag system, thus the rotational speed of the rotor is as can be seen in Fig. 2. However, Fig. 2 is not the second order lag system in a narrow sense. The system of ultrasonic motors is not composed solely of the vibration of the stator. Contact problems and vertical motion of the rotor require consideration. Therefore, the system of ultrasonic motors is more complex in truth.

A. *Effect of frequency*

We conducted the measurement repeatedly changing the frequency of voltage and check the relationship between frequency and static rotational speed, delay time and overshoot of the rotor. The amplitude of the applied voltages and the phase difference are fixed to15Vp-p and 90deg. The results are shown in Fig. 3. Focusing on Fig. 3(a), there is the peak at about 37.1kHz. This frequency is the natural frequency of the motor. The amplitude of the stator and the rotational speed of the rotor is at its highest at this frequency. Fig. 3(b) shows that when the frequency of the applied voltage is near the natural frequency, it takes longer for the rotational speed to settle with little overshoot. The cause of this is difference between the frequency of the applied voltage and the natural frequency of the stator. When the rotor rotates in a transitional condition, the stator vibrates by two frequencies. One is the frequency of the applied voltages and the other is the natural frequency. Vibration by the natural frequency attenuates with time, therefore finally the stator vibrates only by the input frequency. The difference between the two frequencies generates a beat within stator. If the difference between the

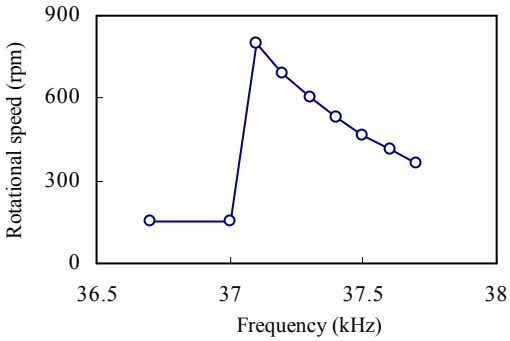

Fig. 3 (*a*) Measured static characteristics

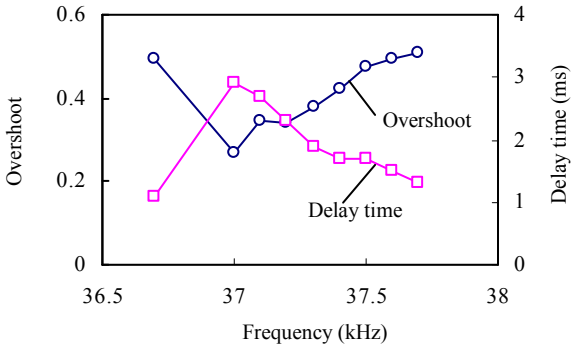

Fig. 3 (*b*) Measured dynamic characteristics

two frequencies is small, the frequency of the beat is small. Rotational speed of the rotor fluctuates at the same frequency of the beat and dynamic characteristics changes.

B. *Effect of amplitude*

As was with frequency response, we measured the history of the rotational speed of the rotor by changing the amplitudes of the applied voltage. The input frequency and the phase difference are fixed to 37.6kHz, 90deg, respectively. Fig. 4 shows the results. Fig. 4(a) shows that amplitude of the voltages is proportional to the rotational speed. Piezoelectric ceramics strain proportionally to the applied voltage, and amplitude of the stator follows the voltage. Therefore the results were as expected. Fig. 4(b) shows that when applied voltage is large, the delay time decreases, the overshoot increases. This tendency resembles the step response of spring-mass-damper system. Spring-mass-damper system is almost the same as the system of the stator and the results resemble each other.

C. *Effect of phase difference*

We next measured the history of the rotational speed of the rotor changing the phase difference. The frequency and amplitude of the voltage are fixed to 37.6kHz, 20Vp-p. Fig. 5 shows the results. Static speed is maximum when the phase difference is 90deg. If the phase difference is 0deg, the vibration of the stator becomes a standing wave and the rotor doesn't move. As the phase difference is near 90deg, the vibration of the stator is proper traveling wave, and the rotational speed increase. Additionally, we can say that as the phase difference gets closer to 90deg, the overshoot decreases, but the delay time doesn't change by changing the phase difference. When the phase difference is approximately 0deg, the amplitude and the propagation

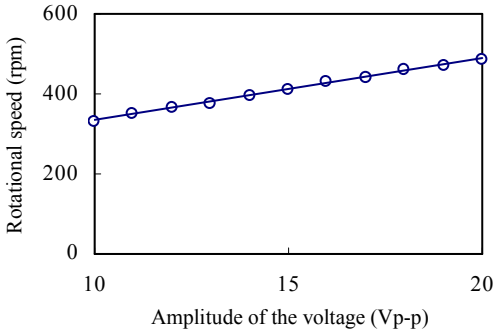

Fig. 4(*a*) Measured static characteristics

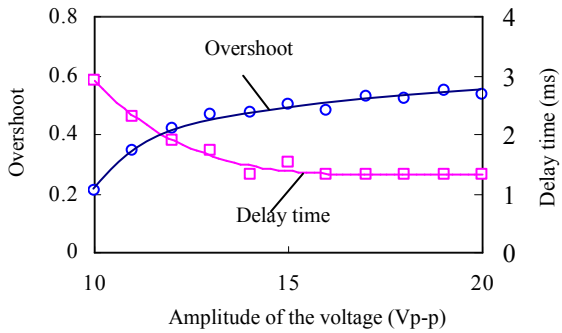

Fig. 4(*b*) Measured dynamic characteristics

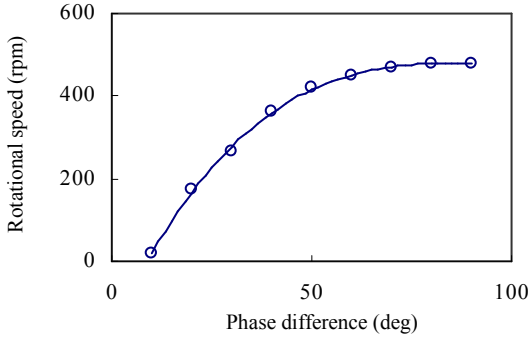

Fig. 5(*a*) Measured static characteristics

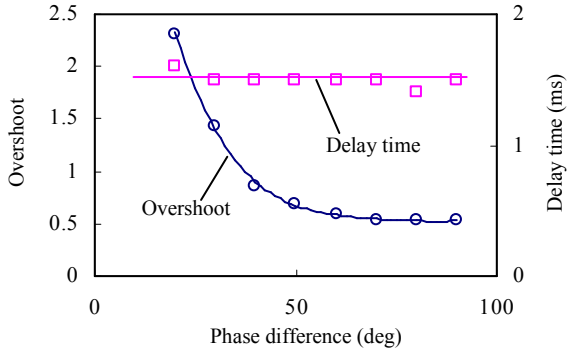

Fig. 5(*b*) Measured dynamic characteristics

speed of the stator gets inhomogeneously even when the stator vibrates in a static region. Thus the vibration of the stator doesn't grow smoothly in the transient region, and the distribution of the propagation speed of the stator is large. Therefore the rotational speed settled with a large overshoot.

IV. Numerical Simulation

In the previous section, we described the measurement of the transient response of bar-type ultrasonic motor. The actual phenomenon of the rotational speed of the rotor was achieved. However, it is inevitable to understand the details of the driving force. In the experiment, we cannot know what happens at the contact area between the rotor and stator. In order to realize high speed control of ultrasonic motors, the contact problem that affects materially the dynamic characteristics and is difficult to measure, must be clarified. To bring out these problems, we conducted numerical simulation based on a mathematical model.

A. Mathematical Modeling

The driving mechanism of ultrasonic motors is divided into three steps as shown in Fig. 6. Part A is the electro-mechanical conversion. In this part, we applied voltage to the piezoelectric ceramics in order to generate moment on the stator. Part B is the stator-vibration part, where the moment is generated on the stator in order to produce vibration in the stator. Part C is the contact part. Friction force is generated between the rotor and the stator. The rotor is driven by the friction force.

In this mechanism, it is important that each part interacts with each other. The interaction of each part must be considered to compute the transient response of the motor.

We constructed a mathematical model as the mechanical part of bar-type ultrasonic motors (part B and part C). Fig. 7 shows the schematic of the model. The model is constructed of three parts. One is the stator model, another is the contact model, and the other is the rotor model.

In the stator model, we account the stator as the rigid disc, torsional spring and damper around three axes. The inertia of the stator and the stiffness of the tosional spring are decided as the natural frequency of the stator becomes 36.5kHz which is measured using LDV. The coefficient of the damper is decided as the Q value of the stator becomes 200, that is measured using LDV. When moment is applied to the stator, the stator vibrates around three axes.

In the contact model, we set the 256 nodes around the top of the stator with equal interval. The rotor and stator affect each other through these nodes. Friction force is generated by the linear springs set around the bottom of the rotor. At all the point of the rotor, three springs are arrayed serially in three directions. If the stator vibrates and some nodes are in contact with the rotor, the spring is compressed by the nodes, therefore reaction force is generated. If stick occurs at the point, the friction force is the same as the reaction force. However, if slip occurs at the node, the friction force will not be the same. Therefore we calculated the friction force by the Coulomb friction rule as follows:

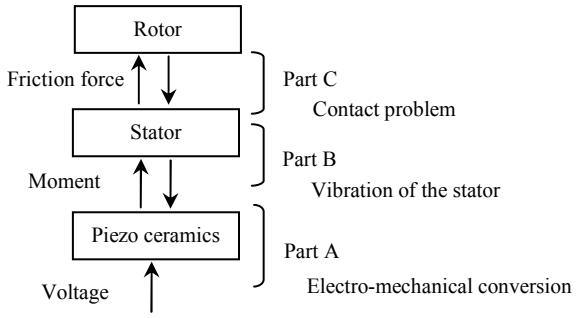

Fig. 6 Mechanism of driving ultrasonic motor

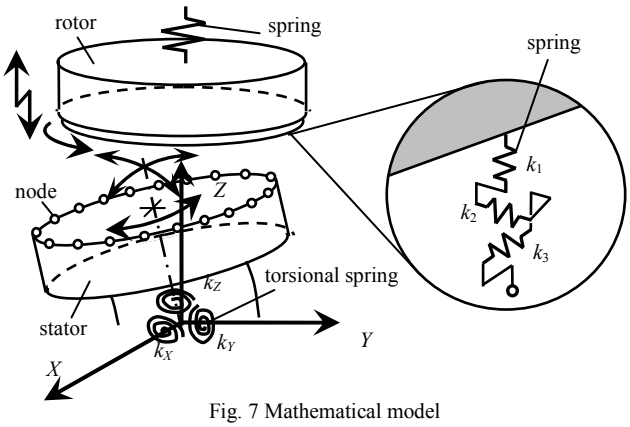

Fig. 7 Mathematical model

$$f = sign\,(v_s - v_r) \cdot \mu_d \cdot F_n \tag{1}$$

Where f is the friction force that is generated at the node, v_s is the tangential velocity of the stator, v_r is the tangential velocity of the rotor, μ_d is the dynamic coefficient of friction, F_n is the normal force at the point. Stick-slip is judged by the following equation (2):

$$f_t > \mu_s \cdot F_n \tag{2}$$

Where f_t is the tangential reaction force when we presume that the slip does not generate at the nodes. μ_s is the dynamic coefficient of friction. If equation (2) is satisfied, we decide that slip generates at the point.

In the rotor model, the rotor is assumed to be driven by the friction force and damping force caused by air viscosity. Motion of the rotor is restricted to the vertical translational motion and the rotation around the Z axis.

The differential equation that describes the behaviors of the motor is shown below.

$$\boldsymbol{I}_s \dot{\boldsymbol{\omega}}_s + \boldsymbol{\omega}_s \times (\boldsymbol{I}_s \boldsymbol{\omega}_s) = \boldsymbol{M}_P - \boldsymbol{M}_E - \boldsymbol{M}_C - \boldsymbol{M}_D \tag{3}$$

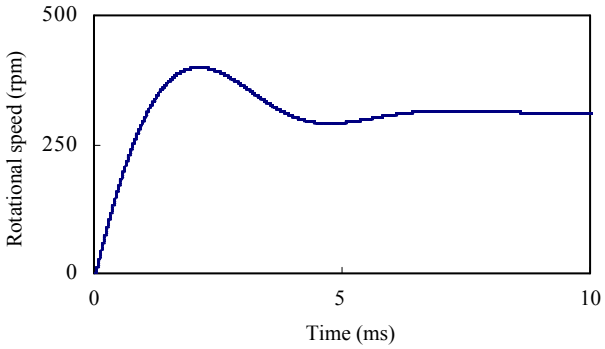

Fig. 8 Calculated history of the rotational speed

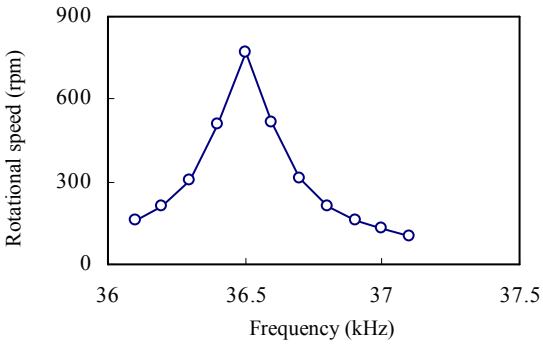

Fig. 9 (*a*) Calculated static characteristics

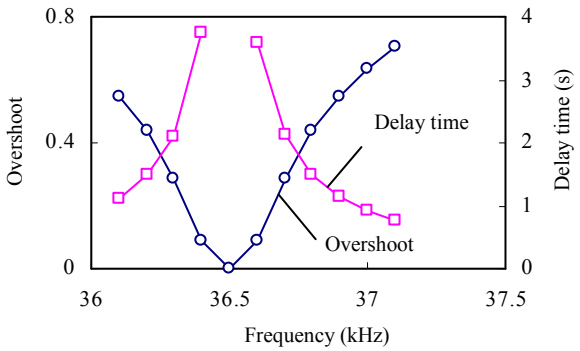

Fig. 9 (*b*) Calculated dynamic characteristics

$$\boldsymbol{I}_r \dot{\boldsymbol{\omega}}_r + \boldsymbol{C}_r \boldsymbol{\omega}_r = \boldsymbol{Mc} \tag{4}$$

$$m_z \ddot{z}_r + c \dot{z}_r + K z_r = F_c \tag{5}$$

Equation (3) describes the motion of the stator. $\boldsymbol{I}_s$ is the inertia of the stator, $\boldsymbol{\omega}_s$ is the angular speed vector of the stator, $\boldsymbol{M}_p$ is the moment from the piezo ceramics, $\boldsymbol{M}_E$ is the moment from elasticity of the stator, $\boldsymbol{M}_C$ is the moment from contact part, and $\boldsymbol{M}_D$ is the moment from damper. Equation (4) describes the rotational motion of the rotor. $\boldsymbol{I}_r$ is the inertia of the rotor, $\boldsymbol{C}_r$ is the damping matrix of the rotor, $\boldsymbol{\omega}_r$ is the angular speed vector of the rotor. Equation (5) describes the vertical motion of the rotor, where m_z is the mass of the rotor, z_r is the vertical position of the rotor, c is the coefficient of damping, K is the stiffness of the spring used for pressing the stator and the rotor, and Fz is the normal force from the stator.

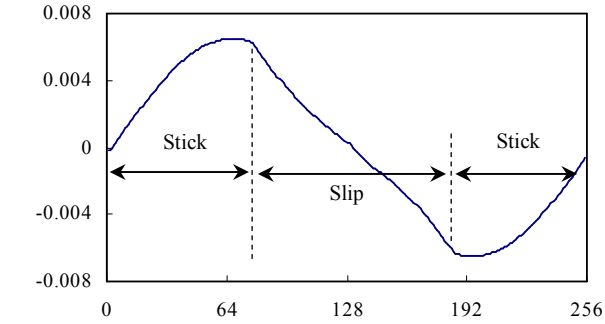

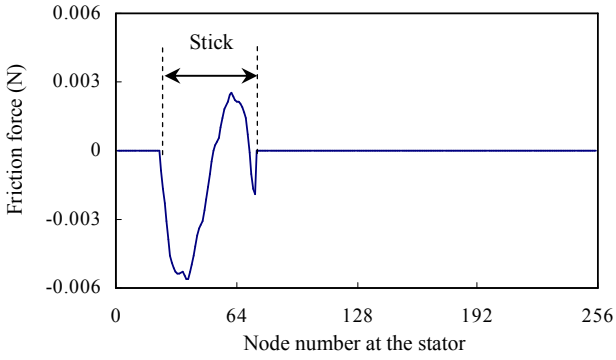

(*c*) t = 3ms

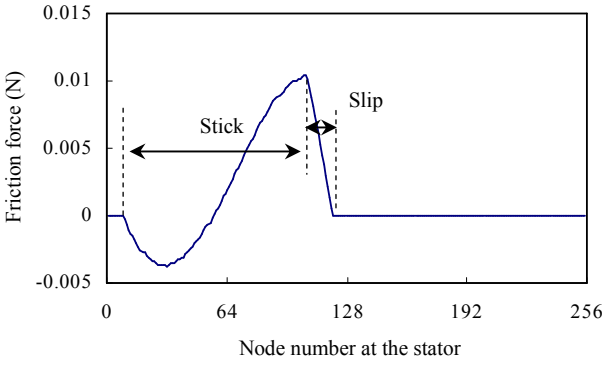

(*b*) t = 0.1ms

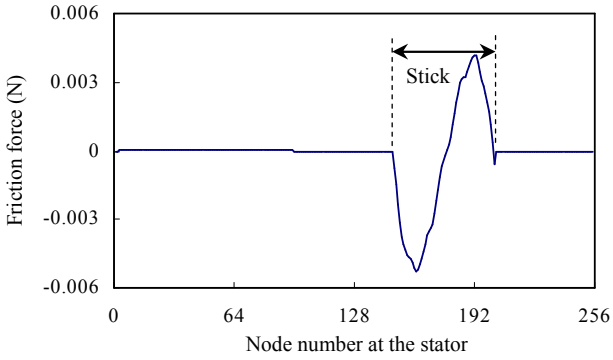

(*d*) t = 4.5ms

Fig. 10 Calculated history of the distribution of the friction force

B. Results

Using the mathematical model, we conducted numerical simulation. Fig. 8 shows the results of calculating the history of rotational speed of the rotor. The frequency, amplitude and phase difference of the applied moment are fixed to 36.7kHz, 0.25N・m and 90deg. The rotational speed of the motor settles in 10ms with overshoot. In this graph, the rotational speed increases in 2ms and settles in 10ms. Though, damping and frequency in damped oscillation are not the same. Therefore Fig. 8 shows the adequacy of the model qualitatively. Calculation was repeated by changing the parameter as was done in the measurements. Fig. 9 shows the frequency response. We fixed the amplitude of the applied moment and the phase difference to be 0.25N・m, 90deg, and changed the frequency of the moment. Static speed of the rotor reached a peak at about 36.5kHz, which is the natural frequency of the stator. As the applied frequency was near the natural frequency, the delay time increased and the overshoot decreased. Compared to Fig. 3, the results of the simulation matched the measure results qualitatively. Therefore, the adequacy of the mathematical model is shown. However, the results of simulation don't match to those of measured quantitatively. The frequency response of the simulation is like that of the linear system. The measured frequency response results seem to be results of non-linear systems. This problem is solved by including non-linear elements in the mathematical model. This will be dealt with in future studies. Next, we consider the contact problem. Because ultrasonic motors are driven by the friction force caused by contact between the rotor and stator, the contact problem greatly affects the dynamics of the motor.

As we described in section 1, the friction force between the rotor and stator is very important. The stator is in contact with the rotor on a line, therefore the friction force is distributed in the contact area. The distribution of friction force changes dynamically, thus it is important to know them. Fig. 10 shows the results of the simulation. Horizontal and vertical axis shows the node number and tangential friction force at the node. 256 nodes are set at the surface of stator and numbered by rotation. t is the time after the moment is applied as an input. Four graphs show the spatial distribution of the friction force at the contact area. Each graph is the result in the discriminative time in the transient region. The driving condition is the same as Fig. 8. The traveling wave is propagated from right to left.

Fig. 10 (*a*) shows the distribution of the friction force after 0.02ms from the time we applied moment to the stator (t =0.02ms). It is the time slightly after we applied the moment. The rotor and the stator are in contact throughout the region, because the amplitude of the stator is small. There is the distribution of stick-slip. Slip occurs at the node where the tangential force is large and the normal force is small. The tangential force is large when the relative speed between the node and the rotor is large. In addition, as shown in Fig. 11, the normal force is small where the normal displacement is small. The rotational speed of the rotor is about 0 rpm and the relative speed is the same as that of the rotor. The orbit of each point is an ellipse and therefore slip tends to occur when the node is at

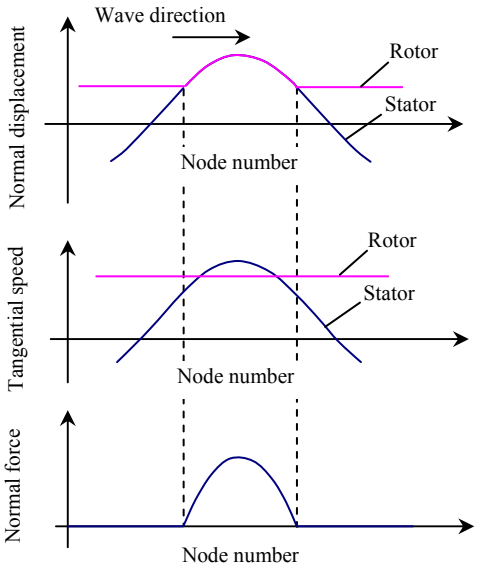

Fig. 11 Relationship between rotor and stator

the bottom of the ellipse.

Fig. 10 (*b*) shows the results when *t* is 0.1ms. This graph shows the distribution of the friction force when the acceleration of the rotor is positive. In this period, the amplitude of the stator grows at some level and contact area is divided into a stick area, slip area and non-contact area. In this condition, as shown in Fig. 11, the normal force is small at the edge of the contact area. The nodes on the left side of the contact area are the nodes which were not in contact with the rotor a moment before. The tangential velocity of the rotor is larger than that of the nodes, and the friction force is negative in this area. However the tangential speed of the nodes increase, shifting to the center of the contact area, and the friction force increases. Just before the nodes part from the rotor, normal force at the nodes decrease and slip occurs. When the speed of the rotor is larger than the average speed of the nodes, and the total friction force is positive.

Fig. 10 (*c*) shows the results when the time is 3ms. Here, the total friction force is negative and the rotor decelerates. There is the stick area throughout the contact area. The amplitude of the stator is large enough and the contact area is smaller than that of Fig. 10 (*b*). Therefore the rotor is in contact only at the top of the elliptical orbit of the nodes. As shown in Fig. 11, the distribution of speed of the nodes at the contact area is small when the contact area is small. Therefore the relative speed (tangential speed) is small throughout the contact area and slip doesn't occur. Here, the speed of the rotor is a little smaller and the total friction force is negative.

Fig. 10 (*d*) shows the distribution of the friction force when the time is 4.5ms. This graph shows the results when the speed of the rotor settles. Just as Fig. 10 (*c*), slip doesn't occur throughout the contact area between the stator and the rotor. The reason of the affinity is the same as Fig. 10 (*c*). The difference between Fig. 10 (*c*) and Fig. 10 (*d*) is the detail in the curve. The reason of this difference is the relative speed between the rotor and stator. The speed of the rotor is about the same as the average speed of the nodes, and the distribution of the friction force is mentioned above.

As we described above, the contact condition and friction force change in the transient region. The factors of these dynamics are the transition of the amplitude of the stator, the relative speed between the rotor and the stator, and the contact area, and so on. Future plans are to correct the model and analyze the dynamics of the motor in further detail. Setting the ultrasonic motor at the joint of the robot hands, we can realize the robots that can accomplish the dexterous task speedier.

V. CONCLUSIONS

In the present study, we measured the step response of the bar-type ultrasonic motor by LDV. In measurement, we changed the parameters of the applied voltages and check the relationship between the applied parameters and the static speed, delay time and the overshoot. Additionally we constructed a mathematical model of a bar-type ultrasonic motor in mechanical part and conducted numerical simulation. The results of the simulation matched the measurement results qualitatively and we could show the adequacy of the model. Using the mathematical model, we computed the contact problem that is difficult to measure and essential to the characteristics of the motor. We calculated the history of the distribution of the friction force and clarified the dynamics at the contact area.

To conduct quantitative analysis, we should introduce nonlinear terms in mathematical model. It is a future plan.

ACKNOWLEDGMENT

This work is supported in part by CANON Inc.

REFERENCES

[1] I. Yamano, K. Takemura, T. Maeno : "Development of a Robot Finger for Five-Fingered Hand usin Ultrasonic Motors", IEEE/RSJ International Conference on Intelligent Robots and Systems, vol. 3 2003, pp 2648-2653

[2] I. Okumura, "A designing method of a bar-type ultrasonic motor for autofocus lenses", *IRToMM-jo International Symposium on Theory of Machines and Mechanisms*, Sep. 1992.

[3] H. Hirata, S. Ueha : "Design of a Traveling Wave Type Ultrasonic Motor", *IEEE Trans. Ultrason., Ferroelect., Freq. Contr.*, vol. 42, no. 2, march 1995

[4] Nesbitt W. Hagood IV, Andrew J. McFarland : "Modeling of a Piezoelectric Rotary Ultrasonic Motor", *IEEE Trans. Ultrason., Ferroelect., Freq. Contr.,* vol. 42, no. 2, pp.210-2124, 1995

[5] M.Tsai, C.Lee, and S.Hwang : "Dynamic Modeling and Analysis of a Bimodal Ultrasonic Motor", *IEEE Trans. Ultrason., Ferroelect., Freq. Contr.,* vol. 50, no. 3, pp.245-255, 2003

[6] Joachim P. Schmidt, P. Hagedorn, and Miao Bingqi : "A Note On The Contact Problem In An Ultrasonic Travelling Wave Motor", *Int. J. Non-Linear Mechanics*, vol. 31, no. 6, pp. 915-924, 1996

[7] S.Gutschmidt, P.Hagedorn : "A Mathematical Model for the Start-up of an Ultrasonic Bar-Type Motor", *Proc., IEEE/ASME, Int., Conf., Adv., Intell., Mechatron.*, vol.2003, no.vol.2, pp 1304-1308, 2003

[8] T. Maeno, T. Tsukimoto, A. Miake : "Finite-Element Analysis of the Rotor/Stator Contact in a Ring Type Ultrasonic Motor", *IEEE Trans. Ultrason., Ferroelec., Freq. Contr,*. vol. 39, no. 6, nov. 1992